International Conference on Automotive Composites
ICAutoC 2016
A. Elmarakbi and A.L. Araújo (Editors)

MULTI-SCALE MODELLING OF GRAPHENE PLATELETS REINFORCED POLYMER MATRIX COMPOSITE MATERIALS

Wiyao Leleng Azoti, Ahmed Elmarakbi

Faculty of Applied Sciences, University of Sunderland, Sunderland, SR6 0DD, UK
wiyao.azoti@sunderland.ac.uk
ahmed.elmarakbi@sunderland.ac.uk

Key words: Graphene composites, Mori-Tanaka scheme, Elasto-plasticity, Lightweighting applications,

Summary: *The use of graphene as polymer reinforcements within composite materials for lightweight purposes is addressed in this work. For that purpose, a multi scale strategy embedding the constitutive law of each phase is accounted for through mean-field technique for obtaining the mechanical properties. Using the Mori-Tanaka micro-mechanics scheme, the effective non-linear behaviour is predicted for various micro-parameters such as the aspect ratio and volume fractions. The results show an enhancement of the equivalent macro stress-strain response with low aspect ratio corresponding to platelets-like inclusions. Also, the volume fraction is seen to improve the composite response. The results compare the contribution of graphene platelets versus that of carbon and glass fibres for lightweight structures with enhanced mechanical responses.*

1 INTRODUCTION

The current pressure growing on automotive manufactures to have strong decarbonisation targets and to reduce annual CO_2 emissions has led to the development of advanced composite materials (ACM) that offer substantial weight reduction while improving strength. The automotive industry, as one of the largest and critical sectors within the global economy, is widely viewed as an area of the greatest volume use for ACM in the future for production of light vehicles. Therefore, the design of the new generation of vehicles should be developed aiming for individual mobility whilst also retaining safety, environmental friendliness and affordability [1]. However, the use of ACM in structural vehicle body applications has been far less extensive [2]. Significant hurdles remain with respect to their improved performance, manufacturability, cost, and modelling [3]. As a consequence, considerable materials science effort and new material discovery need to be developed to overcome these hurdles.
Graphene is at the centre of an ever growing academic and industrial interest because it can produce a dramatic improvement in mechanical properties at low filler content [4]. Indeed, one of the most immediate application for graphene resides in composite materials [5]. To take a full advantage of its properties, integration of individual graphene sheets in polymer matrices is important. Exceptional physical as well as thermomechanical properties, a high

surface/volume ratio and low filler content of graphene make it a promising candidate for developing the next-generation of polymer composites [6-8]. Graphene has been used to increase stiffness, toughness and thermal conductivity of polymer resins by a large margin [9-12]. However, many challenges, including the lack of constitutive material modelling for high performance structural applications can affect the final properties and applications of graphene composites.
In this work, it is aimed to address the constitutive modelling of graphene based polymer composite materials for understanding its contribution in the enhancement of polymer matrix composites for lightweight structural applications. Graphene is considered as platelets embedded within a rate-independent elasto plastic matrix phase. The composite response is therefore computed under a boundary value problem by applying static or kinematic admissible loading. Mean field homogenisation scheme for instance the Mori-Tanaka is used to obtain the overall response of the composite.

2 MEAN FIELD HOMOGENISATION FORMALISM

A macroscopic homogeneous and microscopic heterogeneous materials is selected under a representative volume element RVE as depicted by Figure 1. The associated boundary-value problems are formulated, in the terms of uniform macro field traction vector or linear displacement fields. The RVE is assumed to be in equilibrium and its overall deformation compatible. Also the body forces and inertia term are neglected.

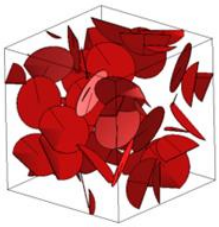

Figure 1: 3D schematics of a RVE of platelets reinforced polymer

These general considerations are restricted to the case of a linear constitutive law under small transformation approximation. They can be summarised like:

$$\sigma_{ij,j} = 0 \tag{1}$$

$$\varepsilon_{ij} = \frac{1}{2}\left(u_{i,j} + u_{j,i}\right) \tag{2}$$

where σ_{ij}, ε_{ij} and u_i represent respectively the components of the stress and strain tensors and the elastic displacement. At each point r in the RVE, the local elastic constitutive law is written such as:

$$\sigma_{ij}(r) = c_{ijkl}(r)\varepsilon_{kl}(r) \tag{3}$$

The scale transition is now introduced to make the relationship between the micro scale (local) and macro scale (global) elastic properties. It consists firstly in the *localisation* step by the global strain tensor $\boldsymbol{A}$ such as:

$$\varepsilon_{ij}(r) = A_{ijkl}(r)E_{kl} \tag{4}$$

The second step of the scale transition is the *homogenisation* which employs averaging techniques to approximate the macroscopic behaviour:

$$\Sigma_{ij} = \frac{1}{V}\int_V \sigma_{ij}(r)\,dV \tag{5}$$

$$E_{ij} = \frac{1}{V}\int_V \varepsilon_{ij}(r)\,dV \tag{6}$$

Replacing Eq. (4) in Eq. (3) and combining the result with Eq. (5), leads to the effective properties given by:

$$C_{ijkl}^{eff} = \frac{1}{V}\int_V c_{ijmn}(r)\,A_{mnkl}(r)dV \tag{7}$$

Or in others terms

$$\boldsymbol{C}^{eff} = \sum_{I=0}^{N} f_I \boldsymbol{c}^I : \boldsymbol{A}^I \tag{8}$$

with $\boldsymbol{c}^I$, $\boldsymbol{A}^I$, f_I the uniform stiffness tensor, the strain concentration tensor and the volume fraction of phase I respectively. Using, the Eshelby's inclusion concept [13], the final expression of the global strain concentration tensor is given by an iterative procedure [14] such as:

$$\begin{cases} \boldsymbol{A}^I = \boldsymbol{a}^I : \left\langle \boldsymbol{a}^I \right\rangle^{-1} \\ \left(\boldsymbol{a}^I\right)_0 = \mathbf{I} \\ \left(\boldsymbol{a}^I\right)_{i+1} = \left(\mathbf{I} + \boldsymbol{T}^{II} : \Delta\boldsymbol{c}^I\right)^{-1} : \left(\mathbf{I} - \sum_{\substack{J=0 \\ J\neq I}}^{N} \boldsymbol{T}^{IJ} : \Delta\boldsymbol{c}^J : \left(\boldsymbol{a}^J\right)_i \right) \\ I = 0,1,2,3,.....,N \end{cases} \tag{9}$$

where $\boldsymbol{a}^I$ states for the local strain concentration tensor and $\Delta\boldsymbol{c}^J = \boldsymbol{c}^J - \boldsymbol{c}^0$. $\boldsymbol{T}^{IJ}$ represents the interaction tensor between inclusions. In the case where the interactions between inclusions are neglected i.e $\boldsymbol{T}^{IJ} = 0$ (most of cases in the open literature), the local concentration tensor $\boldsymbol{a}^I$ reads more simple expression:

$$\boldsymbol{a}^I = \left[\mathbf{I} + \boldsymbol{T}^{II} : \Delta\boldsymbol{c}^{\,I}\right]^{-1} = \left[\mathbf{I} + \mathbf{S} : \left(\boldsymbol{c}^0\right)^{-1} : \Delta\boldsymbol{c}^{\,I}\right]^{-1} \tag{10}$$

where $\mathbf{S}$ represents the Eshelby's tensor [13]. Its expression depends on the aspect ratio $\alpha = c/a$ of the ellipsoidal inclusion of semi-axis (a,b,c) and the material properties of the surrounding matrix $\boldsymbol{c}^0$. Under the Mori-Tanaka MT [15] assumptions, the global strain concentration tensor of the matrix is expressed as [14, 16]:

$$\boldsymbol{A}^0 = \boldsymbol{a}^0 : \left\langle \boldsymbol{a}^I \right\rangle^{-1} = \left(f_0\mathbf{I} + \sum_{I=1}^{N} f_I \boldsymbol{a}^I \right)^{-1} \tag{11}$$

leading to the effective MT properties through Eq. (8) such as:

$$\boldsymbol{C}^{MT} = \sum_{I=0}^{N} f_I \boldsymbol{c}^I \boldsymbol{A}^I = \left(f_0 \boldsymbol{c}^0 + \sum_{I=1}^{N} f_I \boldsymbol{c}^I \boldsymbol{a}^I \right) : \boldsymbol{A}^0 \tag{12}$$

3 DERIVATION OF NON LINEAR TANGENT OPERATORS

Within the RVE, let us assume that one or more phases behave elasto-plastically. Referring to the work by Doghri and Ouaar [17] at least two tangent operators can be defined: the "continuum" (or elasto-plastic) $\boldsymbol{C}^{ep}$ tangent operator, which is derived from the rate constitutive equation, and the "consistent" (or algorithmic) $\boldsymbol{C}^{a\lg}$ tangent operator, which is solved by a discretisation in the time interval $\left[t_n,\ t_{n+1}\right]$. These tangent operators are related to the rate of the constitutive equation as follows:

$$\begin{cases} \dot{\boldsymbol{\sigma}} = \boldsymbol{C}^{ep} : \dot{\boldsymbol{\varepsilon}} \\ \delta\boldsymbol{\sigma}_{n+1} = \boldsymbol{C}^{a\lg} : \delta\boldsymbol{\varepsilon}_{n+1} \end{cases} \tag{13}$$

They are derived from the classical J_2 flow rule:

$$\begin{cases} \boldsymbol{\sigma} = \boldsymbol{C}^{el} : \left(\boldsymbol{\varepsilon} - \boldsymbol{\varepsilon}^p \right) \\ f = \sigma_{eq} - R(p) - \sigma_Y \\ \dot{\boldsymbol{\varepsilon}}^p = \dot{p}\boldsymbol{N}, \ \ \boldsymbol{N} = \dfrac{\partial f}{\partial \boldsymbol{\sigma}} = \dfrac{3}{2}\dfrac{dev(\boldsymbol{\sigma})}{\sigma_{eq}} \\ \sigma_{eq} = \left(\dfrac{3}{2} \boldsymbol{s} : \boldsymbol{s} \right)^{1/2} \end{cases} \tag{14}$$

The "continuum" (or elasto-plastic) $\boldsymbol{C}^{ep}$ tangent operator yields:

$$\begin{cases} \boldsymbol{C}^{ep} = \boldsymbol{C}^{el} - \dfrac{(2\mu)^2}{h} \boldsymbol{N} \otimes \boldsymbol{N} \\ h = 3\mu + \dfrac{dR}{dp} > 0 \end{cases} \tag{15}$$

while the "consistent" (or algorithmic) $\boldsymbol{C}^{a\lg}$ tangent operator is given by:

$$\begin{cases} \boldsymbol{C}^{a\lg} = \boldsymbol{C}^{ep} - (2\mu)^2 \, \Delta p \dfrac{\sigma_{eq}}{\sigma_{eq}^{tr}} \dfrac{\partial \boldsymbol{N}}{\partial \boldsymbol{\sigma}} \\ \dfrac{\partial \boldsymbol{N}}{\partial \boldsymbol{\sigma}} = \dfrac{1}{\sigma_{eq}} \dfrac{3}{2} \mathbf{I}^{dev} - \boldsymbol{N} \otimes \boldsymbol{N} \end{cases} \tag{16}$$

In equations (15) and (16), μ denotes the material shear modulus while $\boldsymbol{C}^{el}$ represents the elastic stiffness tensor and $R(p)$ is the hardening stress function with p the accumulated plastic strain. $\boldsymbol{N}$ represents the normal to the yield surface in the stress space. σ_{eq}^{tr} denotes a trial elastic predictor of σ_{eq}. $\mathbf{I}^{dev}$ stands for the deviatoric part of the fourth order symmetric identity tensor. The knowledge of internal variables such as Δp and σ_{eq}^{tr} is important for

computing the algorithmic tangent operator in Eq. (16). A detailed procedure about the update of internal variables can be found in Azoti et al. [18]. $\boldsymbol{C}^{a\lg}$ will be later used to determine the overall composite behaviour using the MT scheme by Eq. (12).

4 NUMERICAL RESULTS AND DISCUSSIONS

The numerical algorithm for solving the overall response of the composite material is shown by Figure 2. The start point of the algorithm is the partition of strain increment $\Delta\boldsymbol{E}$ between the matrix phase and inclusions. To this end, Voigt assumption is used to state the strain increment in the inclusions (GPL) while an average technique expresses the strain increment in the matrix (polymer). Next, the algorithmic tangent operator of each phase is computed using Eq. (16). Due to its robustness, the generalised mid-point rule [17] is applied on the algorithmic tangent operator to derive the global strain concentration tensor $\boldsymbol{A}^I$. Finally, the effective properties are obtained using Eq. (12) after a convergence checking.

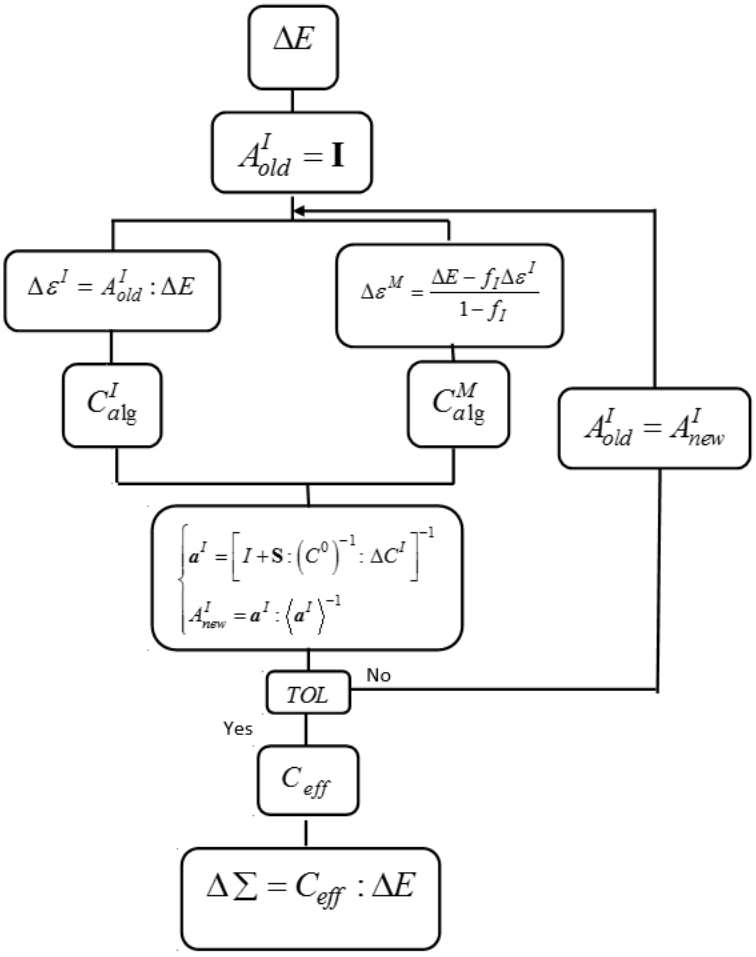

Figure 2: Numerical algorithm for overall response of 2-phases composite

For application, 2-phases composite is considered. The RVE is subjected to uniaxial loading. The load is given in terms of macro stain increment $\Delta\boldsymbol{E} = \Delta\boldsymbol{E}.\psi$ with

$\psi = e_1 \otimes e_1 - \frac{1}{2}\left[e_2 \otimes e_2 + e_3 \otimes e_3\right]$. The matrix is an elasto-plastic Polymer PA6-B3K with an isotropic hardening in power-law $R(p) = kp^m$ whereas the graphene inclusions are considered elastic. The properties of the matrix and the inclusions are reported in Table1

Matrix (Polymer PA6-B3K)					Inclusions (Graphene G2NAN)	
E_0	ν_0	σ_Y	k	m	E_I	ν_I
2000 MPa	0.39	60.5 MPa	63 MPa	0.4	1000 GPa	0.22

Table 1: Phases properties of a Graphene-reinforced polymer composite

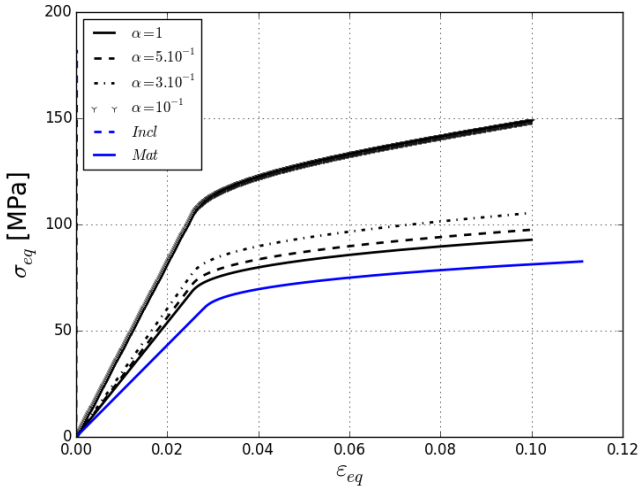

Figure 3: Aspect ratio variation for $f_I = 0.1$

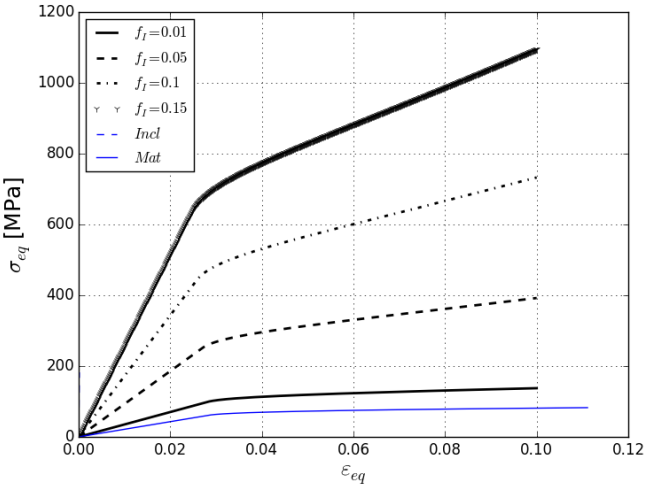

Figure 4: Volume fraction variation for $\alpha = 0.01$

Figure 3 depicts the evolution of the effective equivalent stress-strain behaviour versus the graphene aspect ratio α. For different values of α the overall response is well bonded between the responses of the matrix as well as the graphene. Also, it can be observed an increase in the overall response with respect to the decrease of α. Therefore, lower values of

$\alpha = 0.1$ corresponding to *platelets-like* inclusions show a good reinforcement character than *circular-like* inclusions i.e $\alpha = 1$. In addition, the variation of the volume fraction is analysed. The equivalent macro stress-strain response versus different volume fractions $f_I = 0.01; 0.05; 0.1; 0.15$ is shown by Figure 4. The model predictions reproduce a trend similar to that of the matrix. The composite stress-strain response shifts towards higher stresses with the increase of the inclusions volume fraction. An enhancement of the mechanical properties is therefore noticed with the volume fraction. Herein the predicted stress-strain curves are also well bounded between the matrix and inclusions responses. Also, due to its low density and high Young modulus ($\rho_I = 1.06 g/cm^3$; $E_I = 1000$ GPa) compared to its counterpart fillers like carbons fibres ($\rho_{cf} = 1.76 g/cm^3$; $E_{cf} = 240$ GPa) or glass fibres ($\rho_{gf} = 2.6 g/cm^3$; $E_{gf} = 85$ GPa) for nearly same Poisson's ratio, Graphene platelets demonstrate, in Figure 5, an enhancement of the overall mechanical properties at very low volume fraction $f_I = 0.01$. This observation opens ways for consideration GPL in the design of high strength lightweight components and by consequence a promising approach for reducing CO_2 emissions.

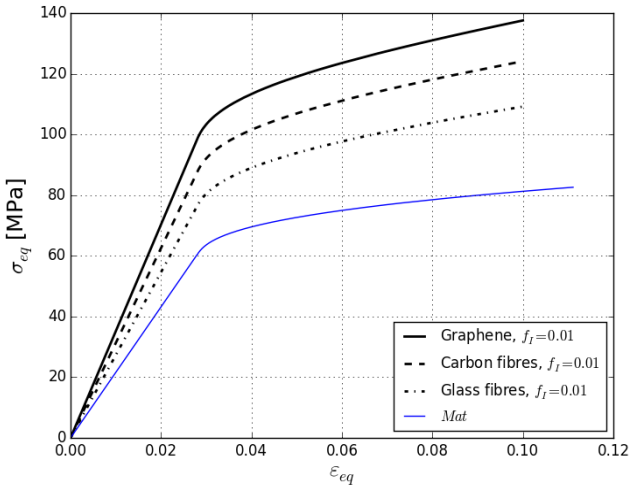

Figure 5: Overall response versus the nature of reinforcement for $\alpha = 0.01$

5 CONCLUSION

The applicability of graphene-based polymer composite materials is made by studying the non-linear effective behaviour of a 2-phases composite. The properties of the graphene are assumed continuous while an elasto-plastic polymer is considered for the matrix. The Mori-Tanaka micro-mechanics scheme derives the effective response of the composite versus the aspect ratio of the graphene sheet and its volume fraction. The results show an enhancement of the equivalent macro stress-strain response with low aspect ratio corresponding to platelets-like inclusions. Also, the volume fraction is seen to have a good improvement on the composite response. With respect to lightweight materials, the results show that GPL are promising candidate and highlight their reinforcement effect versus carbon and glass fibres in the design of lightweight structures with high mechanical responses.

Acknowledgments
The research leading to these results has received funding from the European Union Seventh Framework Program under grant agreement no. **604391 Graphene Flagship**.

REFERENCES

[1] Gundolf Kopp, Elmar Beeh, Roland Scholl, Alexander Kobilke, Philipp Strassburger, and Michael Krieschera. New lightweight structures for advanced automotive vehicles-safe and modular. *Procedia - Social and Behavioral Sciences*, 48 (0): 350 – 362, 2012.
[2] Erica R.H. Fuchs, Frank R. Field, Richard Roth, and Randolph E. Kirchain. Strategic materials selection in the automobile body: Economic opportunities for polymer composite design. *Composites Science and Technology*, 68 (9): 1989 – 2002, 2008.
[3] WilliamJ. Joost. Reducing vehicle weight and improving u.s. energy efficiency using integrated computational materials engineering. *JOM*, 64 (9): 1032–1038, 2012.
[4] Tapas Kuilla, Sambhu Bhadra, Dahu Yao, Nam Hoon Kim, Saswata Bose, and Joong Hee Lee. Recent advances in graphene based polymer composites. *Progress in Polymer Science*, 35 (11): 1350 – 1375, 2010.
[5] Robert J. Young, Ian A. Kinloch, Lei Gong, and Kostya S. Novoselov. The mechanics of graphene nanocomposites: A review. *Composites Science and Technology*, 72 (12): 1459 – 1476, 2012.
[6] Sungjin Park and Rodney S. Ruoff. Chemical methods for the production of graphenes. *Nat Nano*, 4 (4): 217–224, April 2009.
[7] Caterina Soldano, Ather Mahmood, and Erik Dujardin. Production, properties and potential of graphene. *Carbon*, 48 (8): 2127 – 2150, 2010.
[8] M. Inagaki, Y. A. Kim, and M. Endo. Graphene: preparation and structural perfection. *J. Mater. Chem.*, 21: 3280–3294, 2011.
[9] Mohammed A. Rafiee, Javad Rafiee, Iti Srivastava, Zhou Wang, Huaihe Song, Zhong-Zhen Yu, and Nikhil Koratkar. Fracture and fatigue in graphene nanocomposites. *Small*, 6 (2): 179–183, 2010.
[10] L. Monica Veca, Mohammed J. Meziani, Wei Wang, Xin Wang, Fushen Lu, Puyu Zhang, Yi Lin, Robert Fee, John W. Connell, and Ya-Ping Sun. Carbon nanosheets for polymeric nanocomposites with high thermal conductivity. *Advanced Materials*, 21 (20): 2088–2092, 2009.
[11] Zhen Xu and Chao Gao. In situ polymerization approach to graphene-reinforced nylon-6 composites. *Macromolecules*, 43 (16): 6716–6723, 2010.
[12] Wen Ling Zhang, Bong Jun Park, and Hyoung Jin Choi. Colloidal graphene oxide/polyaniline nanocomposite and its electrorheology. *Chem. Commun.*, 46: 5596–5598, 2010.
[13] J. D. Eshelby. The determination of the elastic field of an ellipsoidal inclusion, and related problems. *Proceedings of the Royal Society of London. Series A, Mathematical and Physical Sciences*, 241 (1226): 376–396, 1957.
[14] P. Vieville, A. S. Bonnet, and P. Lipinski. Modelling effective properties of composite materials using the inclusion concept. general considerations. *Arch. Mech.*, 58 (3): 207–239, 2006.
[15] T Mori and K Tanaka. Average stress in matrix and average elastic energy of materials

with misfitting inclusions. *Acta Metallurgica*, 21 (5): 571 – 574, 1973.

[16] W.L. Azoti, Y. Koutsawa, A. Tchalla, A. Makradi, and S. Belouettar. Micromechanics-based multi-site modeling of elastoplastic behavior of composite materials. *International Journal of Solids and Structures*, 59: 198 – 207, 2015.

[17] I. Doghri and A. Ouaar. Homogenization of two-phase elasto-plastic composite materials and structures: Study of tangent operators, cyclic plasticity and numerical algorithms. *International Journal of Solids and Structures*, 40 (7): 1681 – 1712, 2003.

[18] W.L. Azoti, A. Tchalla, Y. Koutsawa, A. Makradi, G. Rauchs, S. Belouettar, and H. Zahrouni. Mean-field constitutive modeling of elasto-plastic composites using two (2) incremental formulations. *Composite Structures*, 105: 256–262, 2013.